

Time- and temperature-dependent domain evolutions in poled (111)-cut $(\text{Pb}(\text{Mg}_{1/3}\text{Nb}_{2/3})\text{O}_3)_{0.7}(\text{PbTiO}_3)_{0.3}$ single crystal

K. S. Wong and J. Y. Dai^{a)}

Department of Applied Physics, The Hong Kong Polytechnic University, Hung Hom, Kowloon, Hong Kong, People's Republic of China

X. Y. Zhao and H. S. Luo

State Key Laboratory of High Performance Ceramics and Superfine Microstructure, Shanghai Institute of Ceramics, Chinese Academy of Science, 215 Chengbei Road, Jiading, Shanghai 201800, People's Republic of China

(Received 15 January 2007; accepted 19 March 2007; published online 20 April 2007)

Ferroelectric domain evolution in poled (111)-cut $(\text{Pb}(\text{Mg}_{1/3}\text{Nb}_{2/3})\text{O}_3)_{0.7}(\text{PbTiO}_3)_{0.3}$ single crystal has been studied by means of piezoresponse force microscopy (PFM). A time-dependent development of lamellar ferroelectric domains from a single domain structure of the just-poled sample has been observed, and it reveals that the formation of the lamellar macrodomains is via the accumulation of well-aligned speckle-shaped nanodomains grown from polar nanosized regions (PNRs). The domain evolutions from macrodomain to microdomain, and from ferroelectric to paraelectric phase at different temperatures, have been revealed in temperature-dependent PFM imaging, and the results are consistent with temperature-dependent relative permittivity measurement. PNRs are believed to play a key role in the domain evolution of depolarization process. © 2007 American Institute of Physics. [DOI: 10.1063/1.2728745]

Relaxor-based ferroelectric crystals, e.g., $(\text{Pb}(\text{Mg}_{1/3}\text{Nb}_{2/3})\text{O}_3)_{1-x}(\text{PbTiO}_3)_x$ (PMN-*x*PT), are important for electromechanical applications ranging from sensors, ultrasound transducers, and actuators because of their high piezoelectric coefficient ($d_{33} \sim 2000$ pC/N) and electromechanical coupling factor ($k_{33} \sim 92\%$).^{1,2} This system is marked by a diffused phase transition in a wide temperature range with a frequency-dependent dielectric constant maximized at temperature T_m which represents the transition temperature from ferroelectric to paraelectric phase. PMN-*x*PT has the complex perovskite structure with an ABO_3 -type unit cell and morphotropic phase boundary in the range of $x = 28\% - 36\%$ of PT.³ A temperature- or electric field-induced phase transition from rhombohedral to monoclinic phase has been found in the morphotropic phase boundary of relaxor materials by means of synchrotron x-ray diffraction, x-ray diffraction reciprocal mapping, neutron diffraction, etc.⁴⁻⁸ The remarkable piezoelectric properties of relaxor ferroelectric materials are considered to be due to the phase transition via the polarization rotation⁹ in the crystal.

Lead magnesium niobate is one of the most interesting relaxor materials and has an ordered-disordered complex structure which is the source of the local random field in $\text{Pb}(\text{Mg}_{1/3}\text{Nb}_{2/3})\text{O}_3$. Lead titanate is a normal ferroelectric material with a long-range order domain structure and has a sharp phase transition at Curie temperature. PMN-*x*PT is the solid solution of $\text{Pb}(\text{Mg}_{1/3}\text{Nb}_{2/3})\text{O}_3$ and PbTiO_3 , in which the substitution of Ti^{4+} cations in *B* sites tends to reduce the random field and enhances the formation of long-range ordered ferroelectric domains.

The evolution of domain structure under different temperatures and electric fields has attracted a great deal of attention, and recently there has been an increasing interest in studying the ferroelectric domains by means of piezore-

sponse force microscopy (PFM). The study of domain structures in relaxor ferroelectrics, e.g., PMN-*x*PT, via PFM has been reported.^{1,10-14} We have also reported the lamellar macrodomains in the poled (111)-cut PMN-30%PT single crystal.¹⁴ However, there is no report on how the lamellar macrodomains is developed from a poled single domain structure in the depolarization process. In this letter, we report the investigation of domain evolution and structure in the poled (111)-cut PMN-30%PT single crystal upon aging and temperature increasing by means of piezoresponse force microscopy.

The PMN-30%PT single crystal was grown by using the modified Bridgman technique.¹⁵ The seed crystal was used along the $\langle 111 \rangle$ direction for growth, and the major face of sample was cleaved as normal to the $\langle 111 \rangle$ direction so it is called (111)-cut single crystal. For measuring the temperature dependence of relative permittivity, the samples with an area of 2 mm^2 and thickness of 1 mm were coated with Cr/Au on both sides as electrodes. In order to investigate the domain structure, the sample was poled along the $\langle 111 \rangle$ direction by an electric field of 10 kV/cm at 110 °C for 20 min and 5 kV/cm in the cooling process. The temperature dependence of relative permittivity of as-grown and poled samples with different frequencies was measured using an impedance analyzer (HP4194A) equipped with a temperature chamber (Delta 9023).

To avoid superposition of domains during PFM imaging, the (111)-cut PMN-30%PT samples were mechanically polished to optical quality with the thickness of about 20 μm . The presence of skin effect in relaxor-based ferroelectric materials has been reported.¹⁶⁻¹⁸ In order to minimize the skin effect and release the stress formed in polishing process, the samples had been annealed at 170 °C ($>T_m$) for 60 min before PFM imaging and poling. The domain images were obtained by piezoresponse force microscope (Nanoscope IV, Digital Instruments, CA) utilizing a conductive tip coated with Cr/Pt. During PFM imaging, a modulating voltage of

^{a)} Author to whom correspondence should be addressed; electronic mail: apdaijy@inet.polyu.edu.hk

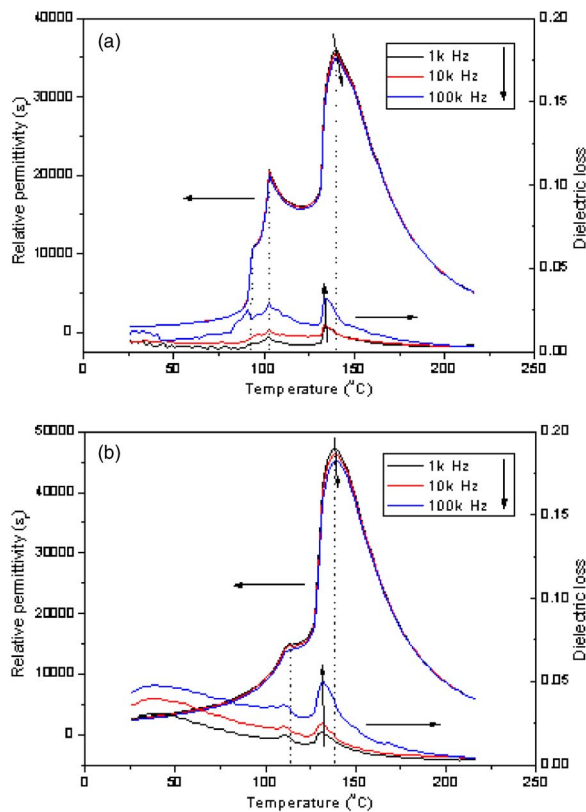


FIG. 1. (Color online) Temperature-dependent relative permittivity and dielectric loss curves for the (111)-cut PMN-30%PT single crystal upon heating: (a) poled and (b) as-grown samples.

4 V (peak to peak) with 11 kHz was applied to Cr/Au bottom electrode, while the tip was electrically grounded.

The curves of temperature-dependent relative permittivity and dielectric loss of the as-grown and poled samples upon heating are shown in Fig. 1. From the two relative permittivity curves, the temperature of maximum dielectric constant, T_m , is determined to be around 139 °C at which the ferroelectric to paraelectric phase transition takes place. For the poled sample, besides T_m , there are another two transition temperatures ~ 93 and ~ 103 °C as shown in Fig. 1(a). According to the phase diagram⁸ of PMN- x PT, 93 °C should be corresponding to a phase transition from ferroelectric rhombohedral (FE_r) to ferroelectric monoclinic (FE_m) phase, and the transition temperature at 103 °C can be attributed to the phase transition from FE_m to ferroelectric tetragonal (FE_t) phase. In contrast, the as-grown sample only possesses transition from FE_r to FE_t phase at 113 °C besides T_m . It is believed that the absence of dispersion in the relative permittivity curve of the poled sample in low temperature range is due to the domination of macrodomains, while the dispersion for the as-grown sample is related to the presence of a large number of polar nanosized regions (PNRs) and microdomains.

Figure 2 shows the piezoresponse phase images of the poled (111)-cut PMN-30%PT single crystal in out-of-plane direction at room temperature. For the just-poled sample, it is apparent that there is no contrast to be observed in the PFM image [Fig. 2(a)], indicating a single domain structure with downward polarization due to successful poling. However, this single domain structure is not energetically stable, and usually depolarization will occur upon increasing of time.

After 5 days, PFM observation reveals some speckle-shaped

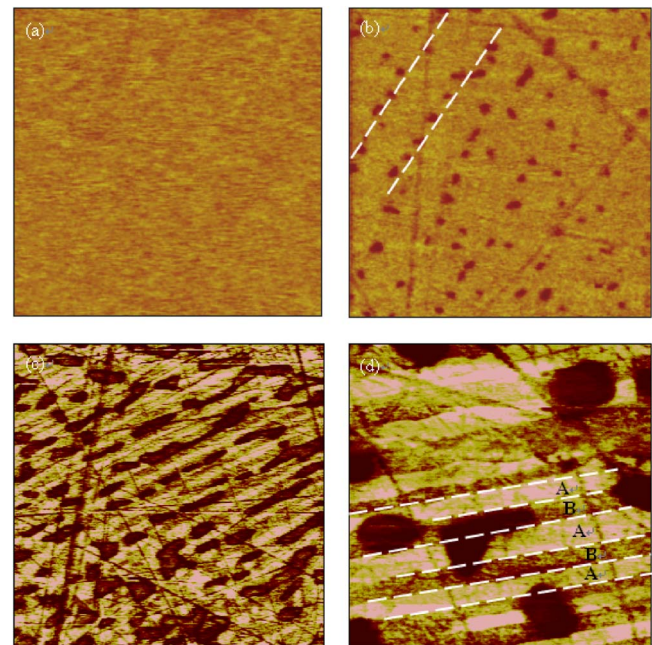


FIG. 2. (Color online) Piezoresponse phase images of the poled (111)-cut PMN-30%PT single crystal after poling process: (a) 1 day (5 μ m scan size), (b) 5 days (20 μ m scan size), and 60 days with (c) 20 and (d) 5 μ m scan sizes.

domains with dark contrast which are well aligned along the straight lines as shown in Fig. 2(b). These speckle-shaped domains with size of around 250–450 nm in diameter are believed to be grown from PNRs. After 60 days, it can be found that the speckle-shaped nanodomains accumulate into lamellar macrodomains having the width of about 1 μ m with different lengths shown as dark contrast regions in the phase images [Figs. 2(c) and 2(d)]. All images in Fig. 2 are captured from the nearby region, and the whole sample exhibits similar features in different areas. These lamellar domains with dark contrast correspond to the upward polarization (pointing out of the paper); while the regions with downward polarization appear bright.

From Fig. 2(d), two regions with lamellar domains of different contrasts appear alternatively: region “A” with uniform and brighter contrast having downward polarization, and region “B” with presence of dark contrast PNRs. We believe that the PNRs play an important role via poling their surrounding lattice in the depolarization process, in which the single domain structure of the just-poled single crystal develops into the lamellar macrodomain structure via the accumulation of backward-polarized PNRs and the speckle-shaped nanodomains. This provides an understanding of depolarization process in the viewpoint of domain evolution. Nevertheless, the reason of the alternative lamellar domain structure with (region B) and without (region A) PNRs as shown in Fig. 2(d) is not very clear, but it may be attributed to the existence of the easy depolarization planes with lower threshold energy for the PNR formation.

In order to understand the relationship between the domain switching and ferroelectric/piezoelectric properties, the time-dependent relative permittivity for 10 kHz and piezoelectric coefficient are measured (not shown) during aging after the sample has been poled. It can be seen that the relative permittivity increases from 880 (just-poled) to 1030 after 30 days, while it is around 2350 for the unpoled sample.

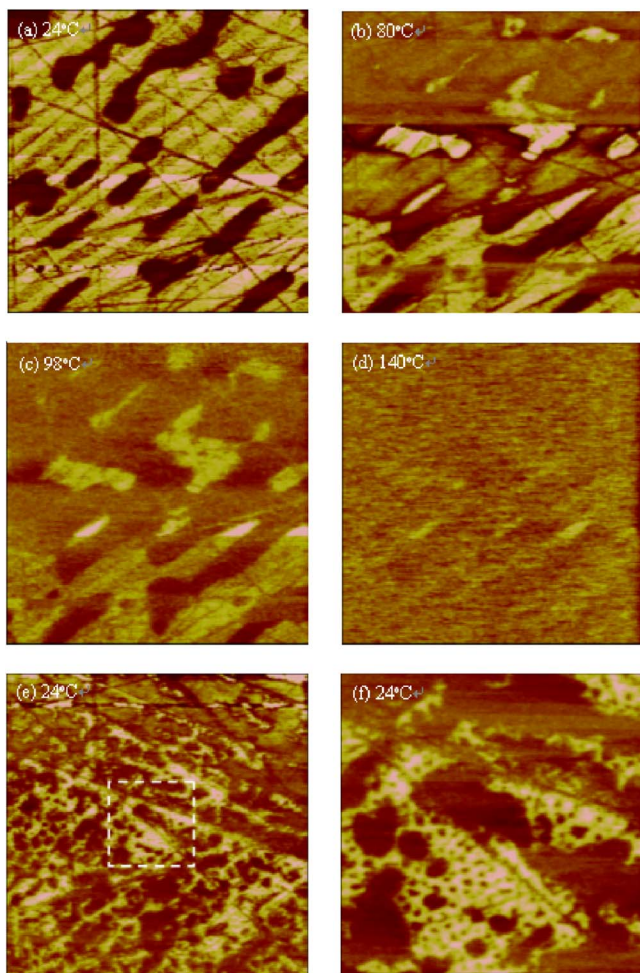


FIG. 3. (Color online) Domain evolution of temperature-dependent piezoresponse phase images in the poled (111)-cut PMN-30%PT single crystal with scan size of $10\ \mu\text{m}$ upon heating: (a) 24, (b) 80, (c) 98, and (d) $140\ ^\circ\text{C}$; (e) piezoresponse phase image with scan size of $10\ \mu\text{m}$ after the sample cool down to room temperature; (f) the magnified image of the outlined region in (e).

After 30 days, the piezoelectric coefficient decreases from 89 to about $65\ \text{pC/N}$. Therefore, it can be concluded that the just-poled (111)-cut PMN-30%PT crystal undergoes depolarization process upon increasing of time in order to reach a steady state. This can be attributed to the back switching of ferroelectric domains in the crystal during aging.

Temperature-dependent piezoresponse force microscopy of the poled (111)-cut PMN-30%PT single crystal upon heating was also carried out after the sample has been aged for 60 days. Figures 3(a)–3(d) show the PFM phase images at 24, 80, 98, and $140\ ^\circ\text{C}$, respectively. All the images in Fig. 3 are obtained from the same region with an indication of scratch from polishing. It can be seen from Fig. 3(a) that at room temperature the lamellar domains are well aligned with very sharp contrast. However, when the temperature reaches $80\ ^\circ\text{C}$, the size of the “dark” lamellar domains becomes larger due to polarization switching as shown in Fig. 3(b). This corresponds to a sudden increase of relative permittivity at $80\ ^\circ\text{C}$ in the relative permittivity curve of the poled sample as shown in Fig. 1(a). The rapid increase of relative permittivity during phase transition is believed to be due to the polarization rotation in the crystal.

When the temperature is further increased to $98\ ^\circ\text{C}$, the domain pattern does not change too much, only the contrast of domains decreases and the image becomes blurred [Fig. 3(c)]. At T_m temperature, because the polarization is getting smaller when the ferroelectric to paraelectric phase transition is taking place, no obvious domain pattern can be observed in the PFM image as shown in Fig. 3(d). After the sample has been kept at $170\ ^\circ\text{C}$ for 30 min and cooled down to room temperature, it can be seen that the speckle-shaped domains with micrometer size dominate the domain configuration instead of the lamellar domains, and a large number of PNRs with size of around $20\text{--}60\ \text{nm}$ can be clearly observed as shown in Fig. 3(f).

The characteristic of relaxor ferroelectrics is the presence of PNRs in the crystal below the Burns temperature T_d , which is a few hundred degrees above the T_m . The number of PNRs in the crystal increases during the sample cooling, but at the freezing temperature T_f , which is typically below T_m , the PNRs will be frozen and a sharp decrease of this number occurs due to the merging of smaller PNRs into the larger ones. The same number of PNRs remains at any temperature upon further cooling below T_f .¹⁹ The size of the PNRs around a few nanometers to $18\ \text{nm}$ in the $\text{Pb}(\text{Mg}_{1/3}\text{Nb}_{2/3})\text{O}_3$ and $\text{Pb}(\text{Zn}_{1/3}\text{Nb}_{2/3})\text{O}_3$ crystals has been reported,^{20,21} which is relatively smaller than what we have measured in the PMN-30%PT sample. This may be due to the relatively weaker random field in the PMN-30%PT single crystal compared to $\text{Pb}(\text{Mg}_{1/3}\text{Nb}_{2/3})\text{O}_3$ and $\text{Pb}(\text{Zn}_{1/3}\text{Nb}_{2/3})\text{O}_3$ crystals.

This project is supported by the Hong Kong RGC Grant No. B-Q772.

- ¹X. Zhao, J. Y. Dai, J. Wang, H. L. W. Chan, C. L. Choy, X. M. Wan, and H. S. Luo, *J. Appl. Phys.* **97**, 094107 (2005).
- ²Y. P. Guo, H. S. Luo, K. P. Chen, H. Q. Xu, X. W. Zhang, and Z. W. Yin, *J. Appl. Phys.* **92**, 6134 (2002).
- ³C. S. Tu, C. L. Tsai, J. S. Chen, and V. H. Schmidt, *Phys. Rev. B* **65**, 104113 (2002).
- ⁴G. Xu, Z. Zhong, Y. Bing, Z.-G. Ye, and G. Shirane, *Nat. Mater.* **5**, 134 (2006).
- ⁵H. Cau, J. Li, D. Viehland, and G. Xu, *Phys. Rev. B* **73**, 184110 (2006).
- ⁶H. Cau, F. Bai, N. Wang, J. Li, D. Viehland, G. Xu, and G. Shirane, *Phys. Rev. B* **72**, 064104 (2005).
- ⁷F. Bai, N. Wang, J. Li, D. Viehland, P. M. Gehring, G. Xu, and G. Shirane, *J. Appl. Phys.* **96**, 1620 (2004).
- ⁸B. Noheda, D. E. Cox, G. Shirane, J. Gao, and Z.-G. Ye, *Phys. Rev. B* **66**, 054104 (2002).
- ⁹H. Fu and R. E. Cohen, *Nature (London)* **403**, 281 (2000).
- ¹⁰H. R. Zeng, H. F. Yu, R. Q. Chu, G. R. Li, H. S. Luo, and Q. R. Yin, *Mater. Lett.* **59**, 238 (2005).
- ¹¹F. Bai, J. F. Li, and D. Viehland, *Appl. Phys. Lett.* **85**, 2313 (2004).
- ¹²V. V. Shvartsman and A. L. Kholkin, *Phys. Rev. B* **69**, 014102 (2004).
- ¹³X. Zhao, J. Y. Dai, J. Wang, H. L. W. Chan, C. L. Choy, X. M. Wan, and H. S. Luo, *Phys. Rev. B* **72**, 064114 (2005).
- ¹⁴K. S. Wong, X. Zhao, J. Y. Dai, C. L. Choy, X. Y. Zhao, and H. S. Luo, *Appl. Phys. Lett.* **89**, 092906 (2006).
- ¹⁵H. S. Luo, G. S. Xu, H. Q. Xu, P. C. Wang, and Z. W. Yin, *Jpn. J. Appl. Phys., Part 1* **39**, 5581 (2000).
- ¹⁶B. Noheda, D. E. Cox, G. Shirane, S.-E. Park, L. E. Cross, and Z. Zhong, *Phys. Rev. Lett.* **86**, 3891 (2001).
- ¹⁷G. Xu, H. Hiraka, G. Shirane, and K. Ohwada, *Appl. Phys. Lett.* **84**, 3975 (2004).
- ¹⁸G. Xu, P. M. Gehring, C. Stock, and K. Conlon, *Phase Transitions* **79**, 135 (2006).
- ¹⁹A. A. Bokov and Z.-G. Ye, *J. Mater. Sci.* **41**, 31 (2006).
- ²⁰P. M. Gehring, S. Wakimoto, Z.-G. Ye, and G. Shirane, *Phys. Rev. Lett.* **87**, 277601 (2001).
- ²¹C. Stock, R. J. Birgeneau, S. Wakimoto, J. S. Gardner, W. Chen, Z.-G. Ye, and G. Shirane, *Phys. Rev. B* **69**, 094104 (2004).